Improving the Elevated-Temperature Properties by Two-Step Heat Treatments in Al-Mn-Mg 3004 Alloys

K. LIU, H. MA, and X. GRANT CHEN

In the present work, two-step heat treatments with preheating at different temperatures (175 °C, 250 °C, and 330 °C) as the first step followed by the peak precipitation treatment (375 °C/48 h) as the second step were performed in Al-Mn-Mg 3004 alloys to study their effects on the formation of dispersoids and the evolution of the elevated-temperature strength and creep resistance. During the two-step heat treatments, the microhardness is gradually increased with increasing time to a plateau after 24 hours when first treated at 250 °C and 330 °C, while there is a minor decrease with time when first treated at 175 °C. Results show that both the yield strength (YS) and creep resistance at 300 °C reach the peak values after the two-step treatment of 250 °C/24 h + 375 °C/48 h. The formation of dispersoids is greatly related to the type and size of pre-existing Mg_2Si precipitated during the preheating treatments. It was found that coarse rodlike β'-Mg_2Si strongly promotes the nucleation of dispersoids, while fine needle like β''-Mg_2Si has less influence. Under optimized two-step heat treatment and modified alloying elements, the YS at 300 °C can reach as high as 97 MPa with the minimum creep rate of 2.2×10^{-9} s^{-1} at 300 °C in Al-Mn-Mg 3004 alloys, enabling them as one of the most promising candidates in lightweight aluminum alloys for elevated-temperature applications.

https://doi.org/10.1007/s11663-018-1268-x

I. INTRODUCTION

DUE to the rapid demand from weight-sensitive automotive and aerospace industries for lightweight materials, such as aluminum alloys, on the elevated-temperature applications, Al-Mn 3xxx alloys have been developed to obtain good properties at both room temperature (RT) and elevated temperature, in which the dispersoid-strengthening mechanism plays a significant role.[1–4] Typical industrial applications of Al-Mn 3xxx alloys can be found in the fabrication of the can body used at RT and the heat exchanger applied at elevated temperature.[5,6] In our previous works,[2,3,7–9] the YS and creep resistance at 300 °C of Al-Mn-Mg 3004 alloy were improved by modifying the alloying elements, such as Mn, Fe, and Mo, and the addition of TiB_2 nanoparticles, to optimize the characters of dispersoids, including the size, volume fraction, and distribution. For instance, Mo was introduced in 3004 alloy to increase the volume fraction of dispersoids and reduce the area of the dispersoid-free zone (DFZ), leading to a significant increase in both the strength and creep resistance at 300 °C.[7] On the other hand, the mechanical properties became worse at high Fe content due to its consumption of Mn to form Al_6(MnFe) intermetallics, resulting in less available Mn solutes for the precipitation of dispersoids.[3] Therefore, optimizing the characters of dispersoids is always the key factor to improving the elevated-temperature properties of dispersoid-strengthened aluminum alloys for elevated-temperature applications.

In addition to modifying the alloying elements, the heat treatment was reported to have a significant influence on the precipitation of dispersoids.[1,2,4,10–13] It is found that the dispersoids changed from α-Al(MnFe)Si to Al_6(MnFe) when the temperature of heat treatment was higher than 600 °C in 3003 alloys,[10,12] while only α-Al(MnFe)Si dispersoids were observed in 3004 alloys due to their high Si content.[2] In addition, the volume fraction of dispersoids decreased with increasing homogenization temperature.[1,2,7,11] Conventionally, the Al-Mn 3xxx alloys are classified as non-heat-treatable alloys. The only heat treatment is the homogenization before rolling or extrusion, which is typically carried out at 600 °C for several hours. For newly developed Al-Mn 3xxx alloys, the heat treatment is performed at 375 °C to 450 °C to promote the precipitation of a large number of dispersoids.[2] It is

K. LIU, H. MA, and X.-GRANT CHEN are with the Department of Applied Science, University of Quebec at Chicoutimi, Saguenay QC, G7H 2B1, Canada. Contact email: kun.liu@uqac.ca
Manuscript submitted August 16, 2017
Article published online May 2, 2018.

reported that the volume fraction of dispersoids decreased from 2.95 vol pct after 375 °C/48 h to 1.94 vol pct after 425 °C/48 h, resulting in the decrease of the YS at 300 °C from 78 to 65 MPa in 3004 alloys.[2] Similar tendency was also reported in 3003 alloys that YS at RT decreased from 87 MPa after 375 °C/24 h to 73 MPa after 450 °C/0.5 h.[11]

However, most of the heat treatments performed in the literature are the single-step treatment with a temperature higher than the precipitation temperature of dispersoids in 3xxx alloys (~ 340 °C[2]). On the other hand, it is suggested that the stepwise heat treatment was helpful for the nucleation and distribution of Al_3Zr dispersoids in 7xxx alloys,[14–18] which consist of the preheating treatment at a low temperature as the first step followed by the conventional precipitation treatment at a high temperature. The first preheating treatment was designed to create a favorable condition of Al_3Zr dispersoid nucleation. It is reported that two-step heat treatment can minimize the precipitation-free zones and greatly increase the number density of dispersoids in 7150 aluminum alloy.[15] However, there is no open literature available for the influence of the two-step heat treatment on the evolution of dispersoids and elevated-temperature properties in Al-Mn 3xxx alloys.

In the present work, various two-step heat treatments with the preheating treatments at 175 °C, 250 °C, and 330 °C as the first step followed by the peak precipitation treatment as the second step are applied on Al-Mn-Mg 3004 alloys. The formation of dispersoids during two-step heat treatments is quantitatively analyzed to establish the relationship between the two-step heat treatment, dispersoid precipitation, and the elevated-temperature strength and creep resistance. In addition, the potential of further improvement of elevated-temperature properties under optimized two-step heat treatment and modified chemical composition are demonstrated for Al-Mn 3xxx alloys.

II. EXPERIMENTAL

Two experimental Al-Mn-Mg 3004 alloys were prepared using commercially pure Al (99.7 pct), pure Mg (99.9 pct), Al-25 pct Mn, Al-25 pct Fe, and Al-50 pct Si master alloys. Alloy A is the base alloy with traditional alloying elements, while alloy B is the alloy with modified chemical composition by adjusting Mn, Fe, and Mo alloying elements, designed for enhancing elevated-temperature properties according to the literature.[3,7,8] In each batch, approximately 3 kg of material was prepared in a clay-graphite crucible using an electric resistance furnace. The temperature of the melt was maintained at ~ 750 °C for 30 minutes. The melt was degassed for 15 minutes and then poured into a permanent mold preheated at 250 °C. The dimension of the cast ingots was 30 mm × 40 mm × 80 mm. The chemical compositions of the experimental 3004 alloys analyzed using an optical emission spectrometer are shown in Table I (all of the alloy compositions are in weight percent unless indicated otherwise).

Table I. Chemical Composition of Experimental Alloys in Present Work

	Elements (Wt Pct)					
Alloy	Mn	Mg	Si	Fe	Mo	Al
A (base)	1.26	1.08	0.24	0.56	0	bal
B	1.52	1.11	0.26	0.29	0.28	bal

During the two-step heat treatment, alloy A was first heat treated at 175 °C, 250 °C, and 330 °C for up to 48 hours as the first step followed by water quench and then heated to 375 °C for 48 hours as the second step followed by water quench at RT. The heating rate for all treatments is controlled at 250 °C/h. As a reference, the single-step heat treatment (375 °C/48 h) was also performed to compare with the properties after two-step heat treatments. In addition, the best two-step heat treatment was selected and applied on alloy B to explore the further improvement of elevated-temperature properties.

After heat treatments, the samples were polished for metallographic observations and machined for mechanical and creep tests. To reveal the dispersoids clearly, the polished samples were etched in 0.5 pct HF for 30 seconds. Optical microscopy (OM) and scanning electron microscopy were used to observe the as-cast and heat-treated microstructures. Transmission electron microscopy (TEM) was used to observe the distribution of dispersoids in the dispersoid zone. The thickness of the TEM sample was measured with electron energy loss spectroscopy equipped with TEM. The size and number density of dispersoids were measured using the image analysis on TEM images. In this study, the volume fraction of DFZ was converted from the area fraction of DFZ measured in the image analysis from optical images according to Delesse's principle,[19,20] while the volume fraction of dispersoids was calculated according to the method introduced in the literature[4] and shown in Eq. [1]:

$$V_v = A_d \frac{\overline{KD}}{\overline{KD} + t}(1 - A_{DFZ}) \quad [1]$$

where $\overline{D}$ is the average equivalent diameter of dispersoids, t is the TEM foil thickness, A_d is the area percentage of dispersoids from TEM observation, A_{DFZ} is the area percentage of DFZ from OM measurements, and $\overline{K}$ is the average shape factor of dispersoids.

Additionally, Vickers microhardness, YS, and creep properties were measured after various heat treatments. Among these properties, microhardness was measured at RT, while mechanical property (YS) and creep resistance were tested at 300 °C. The YS at 300 °C was obtained from compression tests at a strain rate of 10^{-3} s^{-1}, which were performed on a Gleeble 3800 (Dynamic Systems Inc., Poestenkill, NY, USA) thermomechanical simulator unit using cylindrical specimens (15 mm in length and 10 mm in diameter). For the compression test at 300 °C, the specimen was heated to the required temperatures with a heating rate of 2 °C/s

and held for 3 minutes to stabilize. An average value of YS was obtained from three tests. The compressive creep tests were performed at 300 °C for 100 hours with a constant load of 45 MPa. The creep specimens were the same size as the Gleeble samples, and three tests were repeated to confirm the reliability of the results at each condition. Details of the test methods can be found in Reference 2.

III. RESULTS AND DISCUSSION

A. *Influence of the Two-Step Treatment on Elevated-Temperature Properties*

Figure 1 shows the evolution of the microhardness of alloy A after two-step heat treatments with the first step at various temperatures followed by 375 °C/48 h. The initial point (0 hours) is the microhardness after the single-step heat treatment (375 °C/48 h). It can be found that the microhardness decreases slightly with time after the two-step heat treatment with the first-step treated at 175 °C compared to the single-step heat treatment. For instance, the microhardness is decreased from 63.5 to 62 HV after treatment at 175 °C/24 h + 375 °C/48 h. However, the microhardness remarkably increases when first treated at both 250 °C and 330 °C, and it reaches the peak value after 12 to 24 hours. Furthermore, the microhardness is higher when treated at 250 °C than at 330 °C at a given holding time. As shown in Figure 1, the value of the microhardness is increased from 63.5 to 66 HV after 330 °C/24 h + 375 °C/48 h and further to 70 HV after 250 °C/24 h + 375 °C/48 h.

In order to evaluate the influence of the two-step treatment on the elevated-temperature properties, the YS and creep properties at 300 °C were measured after two-step heat treatments with various preheating temperatures after 24 hours, and the results are shown in Figure 2. It can be seen that the change of properties after various two-step heat treatments in Figure 2 is similar to the evolution of microhardness in Figure 1. As shown in Figure 2(a), the YS at 300 °C is lower after the two-step heat treatment when first treated at 175 °C (175 °C/24 h + 375 °C/48 h), but it is higher than the single-step treatment (375 °C/48 h) when first treated at 250 °C and 330 °C. For instance, the YS at 300 °C after 175 °C/24 h + 375 °C/48 h is 78.6 MPa, which is lower than that after the single-step heat treatment (79.7 MPa). However, the YS increases to 81 MP after 300 °C/24 h + 375 °C/48. The highest YS at 300 °C is obtained after the two-step heat treatment of 250 °C/24 h + 375 °C/48 h, which reaches 82.7 MPa.

Figure 2(b) shows the typical creep curves after various two-step heat treatments. It can be seen that the creep stain after 175 °C/24 h + 375 °C/48 h is slightly higher than that after the single-step treatment. However, the creep strain is much lower after treatment at 330 °C/24 h + 375 °C/48 h and 250 °C/24 h + 375 °C/48 h. As shown in Figure 2(b), the creep strain decreases from 0.014 after the single treatment (375 °C/48 h) to 0.008 after 330 °C/24 h + 375 °C/48 h and further to 0.0038 after 250 °C/24 h + 375 °C/48 h. The minimum creep rate is calculated to be 3.9×10^{-8} s^{-1} after 175 °C/24 h + 375 °C/48 h, 3.1×10^{-8} s^{-1} after 375 °C/48 h, 1.6×10^{-9} s^{-1} after 330 °C/24 h + 375 °C/48 h, and 7.5×10^{-9} s^{-1} after 250 °C/24 h + 375 °C/48 h. It is evident that the two-step heat treatment of 250 °C/24 h + 375 °C/48 h possesses the lowest creep strain and the lowest minimum creep rate, indicating the best creep resistance among the four heat treatment conditions investigated.

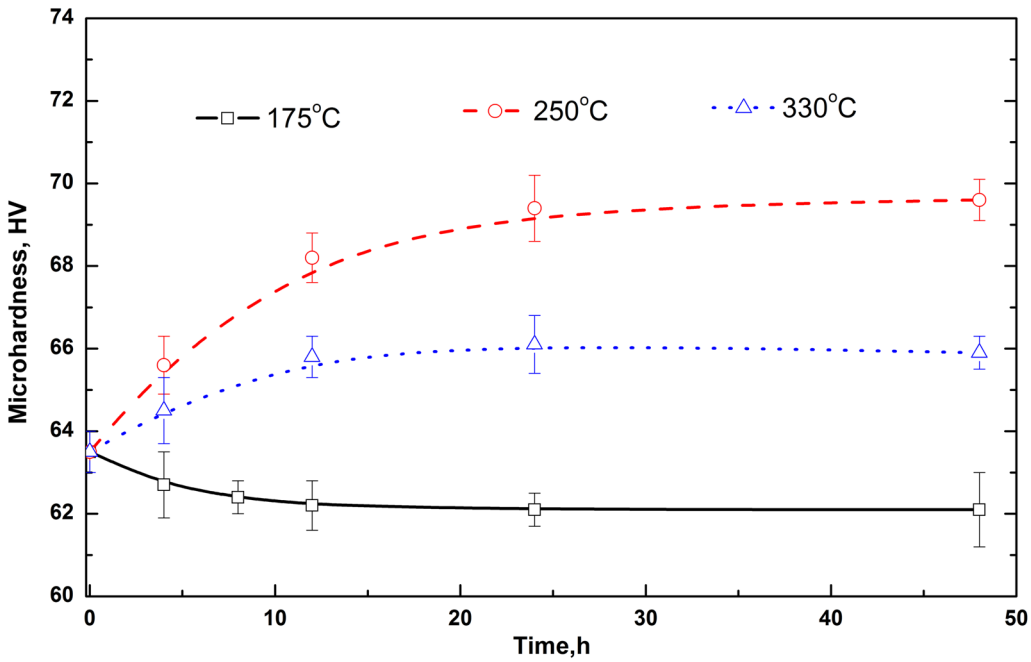

Fig. 1—Evolution of microhardness of alloy A after two-step treatments with the first step at various temperatures.

B. *Evolution of Dispersoids during Two-Step Heat Treatment*

As shown in Figures 1 and 2, the microhardness at RT as well as the strength and creep resistance at 300 °C can be greatly influenced by the two-step heat treatment. It is apparent that the change of elevated-temperature properties is attributed to the evolution of strengthening phase in the microstructure, namely, the precipitation of α-Al(MnFe)Si dispersoids in 3004 alloy during the two-step heat treatment according to the Orowan strengthening mechanism.[4,11,21] The general distribution of dispersoids was first checked with OM, and the results are shown in Figure 3.

It can be found that when pretreated at 250 °C (Figure 3(c)) and 330 °C (Figure 3(d)), there is no obvious change in the distribution of dispersoids with a minor change in the DFZ compared to the single-step treatment (Figure 3(a)). As shown in Figures 3(a), (c), and (d), the dispersoids are uniformly distributed in the dendrite cells with the interdendritic DFZ surrounding the intermetallics (the black Mn-containing intermetallic, arrow marked in Figure 3(b)). In addition, it seems that DFZ is the least in Figure 3(c) after pretreatment at 250 °C. However, when pretreated at 175 °C (Figure 3(b)), the volume of DFZ seems to be higher than the other three conditions but the dispersoids are still uniformly distributed in the center of the dendrites.

In addition, the characteristics of dispersoids in the dispersoid zone after various two-step heat treatments were studied using TEM in more detail and the results are shown in Figure 4. According to TEM–energy-dispersive spectroscopy (EDS) results and the literature,[2,7] all dispersoids found here are α-Al(MnFe)Si dispersoids. Since the dipsersoids have been identified by TEM with the selected area diffraction pattern and EDS in our previous works,[2,7] the TEM–EDS results are not shown in the present work.

Compared to the dispersoids after the single-step heat treatment (375 °C/48 h) in Figure 4(a), the size of dispersoids is larger when pretreated at 175 °C (Figure 4(b)). However, when pretreated at 250 °C (Figure 4(c)), the size of dispersoids generally becomes smaller. When pretreated at 330 °C, the dispersoids have a similar size (Figure 4(d)) with the single-step treatment (Figure 4(a)). Therefore, the finer dispersoids (Figure 4(c)), combined with less area of DFZ (Figure 3(c)) after 250 °C/24 h + 375 °C/48 h, result in the highest strength and creep resistance (Figure 2) as well as the highest microhardness (Figure 1). On the other hand, the larger size of dispersoids (Figure 4(b)) and greater area of DFZ (Figure 3(b)) after 175 °C/24 h + 375 °C/48 h are responsible for the lowest properties.

The different characteristics of α-Al(MnFe)Si dispersoids during various two-step heat treatments can be attributed to the formation of pre-exiting Mg_2Si in the first-step treatment. The pre-exiting Mg_2Si was reported to be the nucleation sites of α-Al(MnFe)Si dispersoids.[22] In the present work, it is observed that, during the heating process toward 375 °C in the single-step treatment, a number of Mg_2Si first precipitated at the temperature range of 150 °C to 300 °C and then slowly dissolved at higher temperatures of 300 °C to 375 °C before the beginning of dispersoid precipitation. The temperature range for the precipitation and dissolution of various Mg_2Si is greatly in accordance with the literature.[23,24] Therefore, two preheating conditions (175 °C/24 h and 250 °C/24 h) are selected to study the relationship between the two-step heat treatment and the dispersoid precipitation. Figures 5(a) and (c) show the microstructure after the first-step treatments, while Figures 5(b) and (d) present the initial state of the dispersoid precipitation, which is after 1 hour at 375 °C.

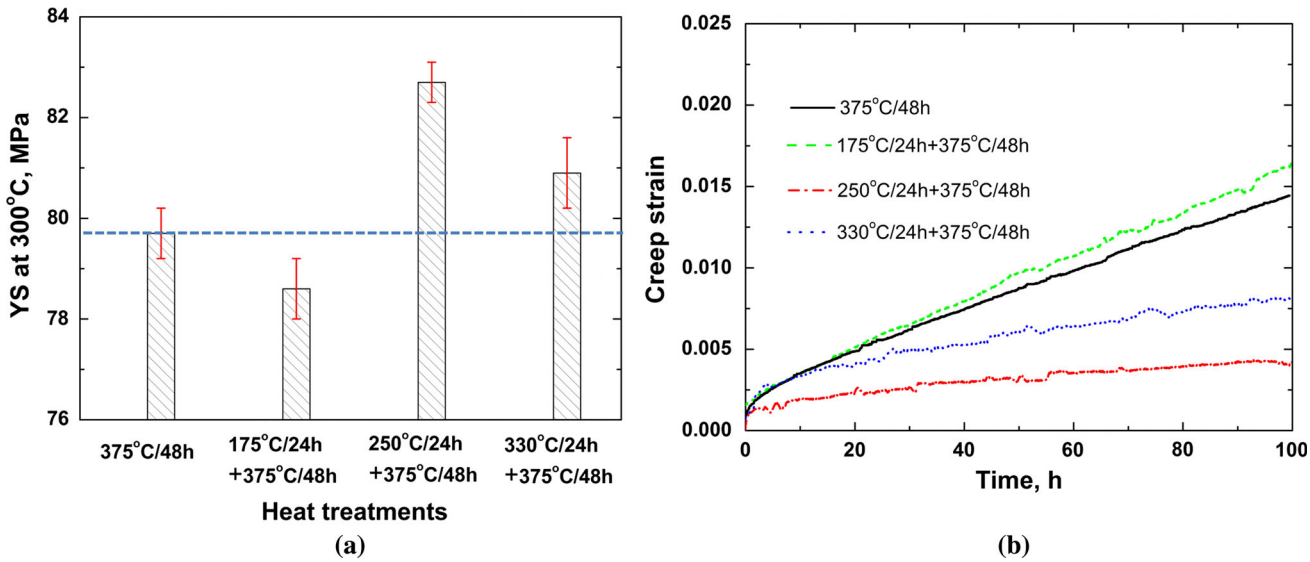

Fig. 2—Evolution of elevated-temperature properties of alloy A after two-step treatments: (*a*) YS at 300 °C and (*b*) typical creep curves at 300 °C.

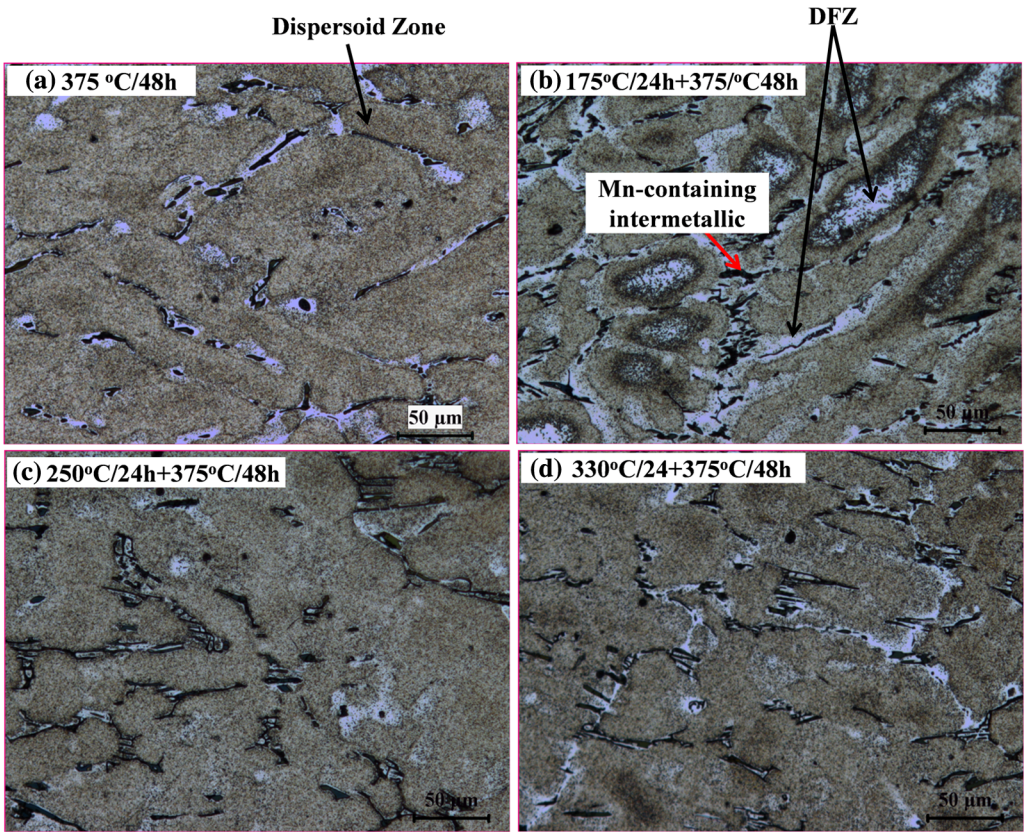

Fig. 3—Microstructure of alloy A after various two-step heat treatments: (*a*) 375 °C/48 h, (*b*) 175 °C/24 h + 375 °C/48 h, (*c*) 250 °C/24 h + 375 °C/48 h, and (*d*) 330 °C/24 h + 375 °C/48 h.

As shown in Figures 5(a) and (c), a large number of Mg_2Si were precipitated at both conditions (175 °C/24 h and 250 °C/24 h). However, there are big differences in the Mg_2Si precipitation, such as the type, size, and morphology. When pretreated at 175 °C/24 h (Figure 5(a)), only very thin needlelike Mg_2Si can be observed and the average size is measured to be 120 (L) × 6 (W) nm, which is reported to be the β''-Mg_2Si.[23,25] On the other hand, Mg_2Si became coarser with thick lath-shaped and rodlike morphology after 250 °C/24 h (Figure 5(c)). The average size was 430 (L) × 26 (W) nm, which is believed to be β'-Mg_2Si, according to the literature.[23–27]

During the second step of heat treatment, the dispersoids begin to form and the orientation is the same with the pre-existing Mg_2Si (Figures 5(b) and (d)), indicating the nucleation and growth of dispersoids on pre-existing Mg_2Si. However, the number density of dispersoids is remarkably different in the two preheating treatments. When pretreating at 175 °C (Figure 5(b)), only a small number of dispersoids can be observed. However, it can be clearly seen that when pretreating at 250 °C (Figure 5(d)), a large number of dispersoids precipitate and all of them align along the original orientation of pre-existing Mg_2Si precipitates. It seems that β'-Mg_2Si with a reasonable size is more appropriate to be the nucleation site of dispersoids than β''-Mg_2Si. In Figures 5(c) and (d), with preheating at 250 °C/24 h, β'-Mg_2Si precipitates with thicker lath-shaped and rodlike morphology show a strong promoting effect on the nucleation of dispersoids, leading to the finer dispersoids and the higher volume of dispersoids formed during the following holding process at 375 °C, as shown in Figure 4(c).

C. *Optimization of Elevated-Temperature Properties of Al-Mn-Mg 3004 Alloy*

As discussed in Section III–A, the proper two-step heat treatment, such as 250 °C/24 h + 375 °C/48 h, can remarkably improve the alloy properties. In addition, our previous works[3,7,8] demonstrated that the elevated-temperature properties of Al-Mn-Mg 3004 alloys can be enhanced by adjusting alloying elements. Alloy B in Table I is designed for an optimized chemical composition by modifying Fe, Mn, and Mo.[3,7,8] Therefore, the two-step heat treatment (250 °C/24 h + 375 °C/48 h) is applied in alloy B to explore the attainable alloy properties at elevated temperature for Al-Mn-Mg 3004 alloys.

The YS values at 300 °C of both alloys A and B after single and two-step heat treatments are shown in Figure 6(a). It can be seen that the YS increases from 80 MPa (alloy A) to 92 MPa (alloy B) after the single-step heat treatment (375 °C/48 h) with modified alloying elements. Furthermore, the YS in alloy B is further improved from 92 MPa after the single-step heat treatment (375 °C/48 h) to 97 MPa after the two-step

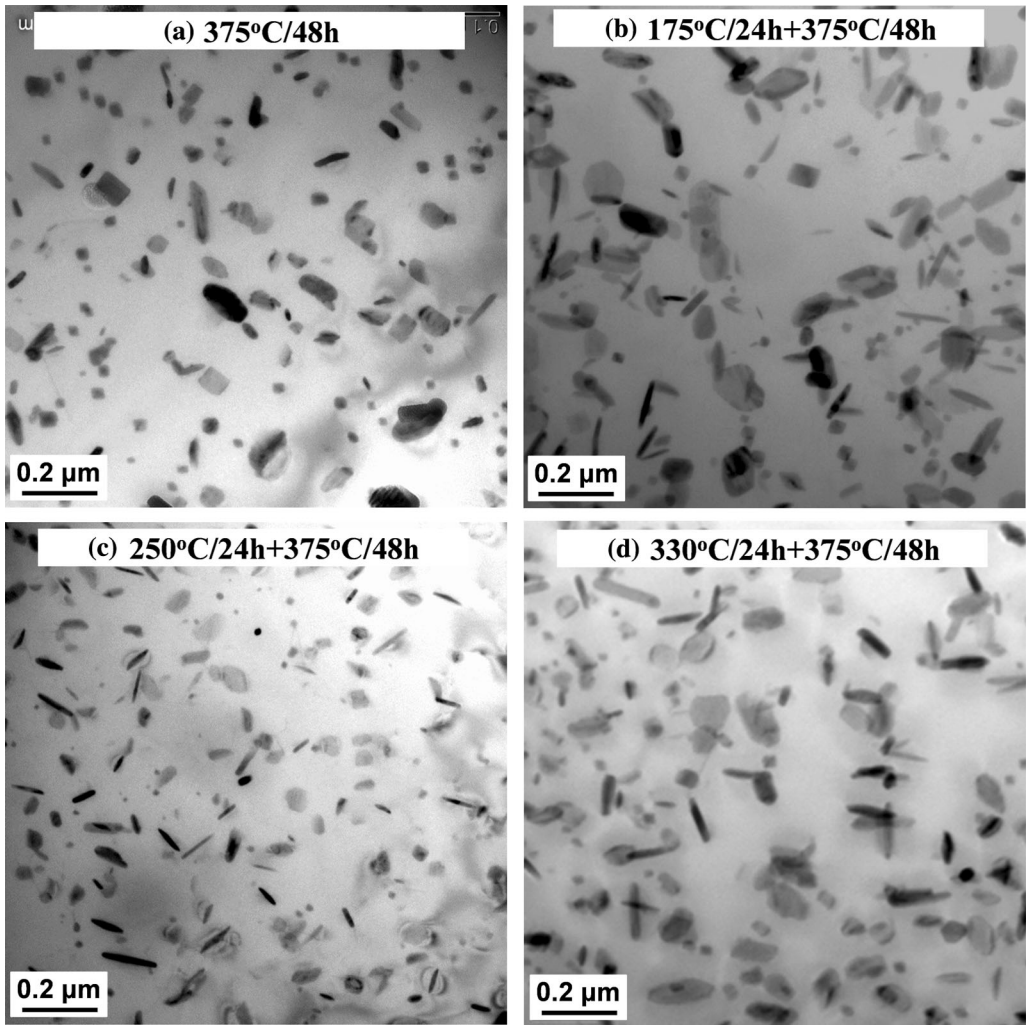

Fig. 4—Distribution of dispersoids after various heat treatments: (*a*) 375 °C/48 h, (*b*) 175 °C/24 h + 375 °C/48 h, (*c*) 250 °C/24 h + 375 °C/48 h, and (*d*) 330 °C/24 h + 375 °C/48 h.

heat treatment (250 °C/24 h + 375 °C/48 h), confirming the synergistic benefit of the two-step heat treatment and modifying alloying elements on enhancing the elevated-temperature properties.

The YS at 300 °C of alloy B after the two-step heat treatment (250 °C/24 h + 375 °C/48 h) can reach as high as 97 MPa (Figure 6(a)), which is 21 pct improvement on the elevated-temperature strength relative to alloy A. It is the maximum attainable YS at 300 °C on Al-Mn-Mg 3004 alloys up to now. To explore the improvement of the creep resistance at elevated temperature, the typical creep curves of these two conditions (alloy B after 250 °C/24 h + 375 °C/48 h and alloy A after 375 °C/48 h) are shown in Figure 6(b). Similar to the YS, the total creep strain dropped from 0.0142 in alloy A after 375 °C/48 h to 0.0025 in alloy B after 250 °C/24 h + 375 °C/48 h during creep deformation of 100 hours at 300 °C. The minimum creep rate decreases from 3.1×10^{-8} s^{-1} (alloy A) to 2.2×10^{-9} s^{-1} (alloy B), which is one order lower on the minimum creep rate.

At the same two-step heat treatment condition (250 °C/24 h + 375 °C/48 h), the total creep stain and the minimum creep rate of alloy A are 0.0038 and 7.5×10^{-9} s^{-1} (Figure 2(b)), respectively. Both the total creep strain and the minimum creep rate of alloy B are lower than those of alloy A. Taking into account both data, this is the best creep resistance obtained in Al-Mn-Mg 3004 alloys. These enhanced elevated-temperature properties after modifications of the heat treatment and alloying elements (alloy B) can be principally attributed to the precipitation of dispersoids (size and volume fraction). Figure 7 shows that the volume fraction of dispersoids in alloy B after 250 °C/24 h + 375 °C/48 h is much higher than that in alloy A after 375 °C/48 h, resulting in the higher elevated-temperature properties in alloy B after 250 °C/24 h + 375 °C/48 h.

Furthermore, those dispersoids in the aluminum matrix are proved to be thermally stable during long-time holding at 300 °C to 350 °C.[2,–7] Therefore, it is expected they will maintain the superior mechanical and creep properties in alloy B even after long-time exposure at high-temperature work conditions (300 °C to 350 °C). This is one of the most significant advantages

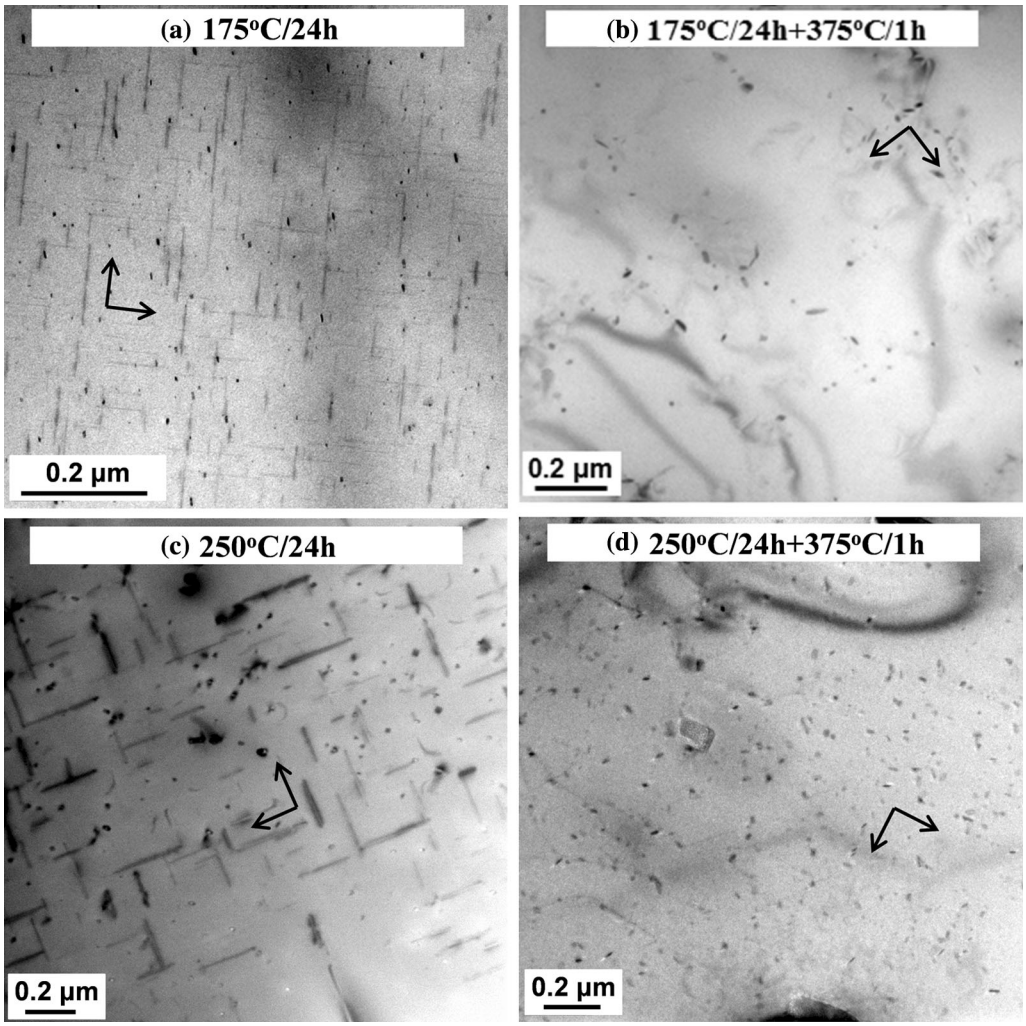

Fig. 5—Microstructure of alloy A at various stages of two-step heat treatments: (*a*) 175 °C/24 h, (*b*) 175 °C/24 h + 375 °C/1 h, (*c*) 250 °C/24 h, and (*d*) 250 °C/24 h + 375 °C/1 h.

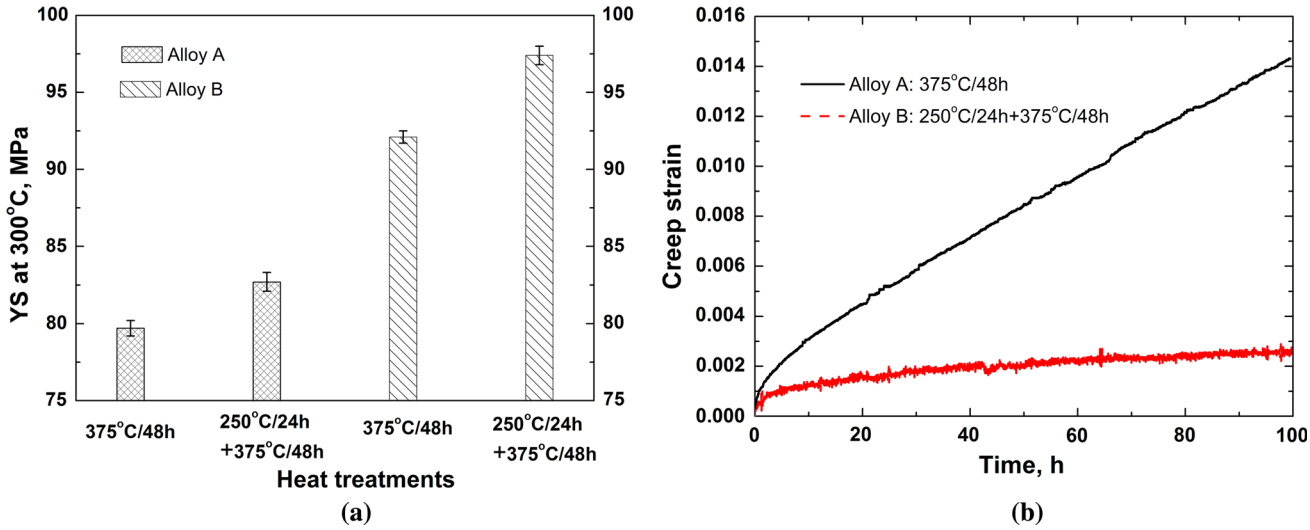

Fig. 6—Elevated-temperature properties of experimental alloys: (*a*) YS at 300 °C and (*b*) typical creep curves at 300 °C.

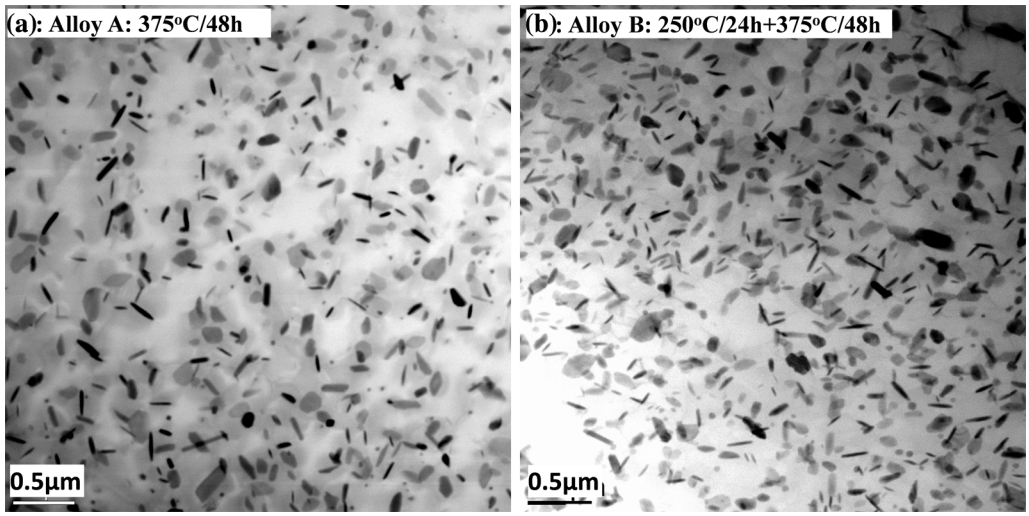

Fig. 7—Precipitation of dispersoids in alloys A and B under different heat treatments: (*a*) alloy A, 375 °C/48 h and (*b*) alloy B, 250 °C/24 h + 375 °C/48 h.

of dispersoid-strengthening aluminum alloys compared to conventional precipitation-hardening aluminum alloys, such as 2xxx, 6xxx, and 7xxx, which exhibit a significant deterioration of mechanical properties during elevated-temperature exposure due to the rapid coarsening of precipitates. For instance, the instant YS at 315 °C of AA2024 after peak aging (T6) is 95 MPa, which is at a similar level of strength as alloy B in the present work, although AA2024-T6 has the highest YS among the precipitation-hardening wrought aluminum alloy.[28] However, the YS at 315 °C of AA2024-T6 rapidly dropped to 45 MPa after exposure for 100 hours at 315 °C, in which 50 pct of YS was lost after thermal holding. Alloy B can still maintain the similar level of YS as that before the thermal exposure during long-term exposure at 350 °C.[7] On the other hand, Al-Mn-Mg 3004 alloys are more economic than other dispersoid-strengthening aluminum alloys with Sc and Zr[29,30] and much lighter than traditional high-temperature alloys, such as Ti and Ni.[31,32] In the practical view, Al-Mn-Mg 3004 alloys are more competitive in large-scale industrial production, which can be processed *via* the conventional ingot metallurgy route and subsequent thermomechanical processes. Therefore, Al-Mn-Mg 3004 alloys with modified alloying elements and optimized heat treatment are one of the most promising candidates in lightweight aluminum alloys for elevated-temperature applications.

IV. CONCLUSIONS

In the present work, the influence of the two-step heat treatment on elevated-temperature properties was investigated in Al-Mn-Mg 3004 alloys, and the following conclusions were drawn.

1. When the first preheating temperature is lower (~ 175 °C), the alloy properties decrease gradually with prolonged holding time, while they increase remarkably when first treated at higher temperatures (250 °C to 330 °C) during two-step heat treatments. The maximum elevated-temperature strength and creep resistance are obtained after the two-step heat treatment of 250 °C/24 h + 375 °C/48 h with finer dispersoids and higher volume fraction of dispersoids.
2. The formation of dispersoids is greatly related to the type and size of pre-existing Mg_2Si precipitated during the first-step treatments, in which coarse rodlike β'-Mg_2Si strongly promotes the nucleation of dispersoids while the fine needlelike β''-Mg_2Si shows less influence.
3. Under optimized two-step heat treatment (250 °C/24 h + 375 °C/48 h) and modified alloying elements (Fe, Mn, and Mo), the YS at 300 °C of Al-Mn-Mg 3004 alloys can reach as high as 97 MPa with the minimum creep rate of 2.2×10^{-9} s^{-1} at 300 °C, making them one of the most promising candidates in lightweight aluminum alloys for elevated-temperature applications.

ACKNOWLEDGMENTS

The authors acknowledge the financial support of the Natural Sciences and Engineering Research Council of Canada (NSERC) and Rio Tinto Aluminum through the NSERC Industry Research Chair in the Metallurgy of Aluminum Transformation at the University of Quebec at Chicoutimi.

REFERENCES

1. Y.J. Li, A.M.F. Muggerud, A. Olsen, and T. Furu: *Acta Mater.*, 2012, vol. 60, pp. 1004–14.
2. K. Liu and X.G. Chen: *Mater. Des.*, 2015, vol. 84, pp. 340–50.

3. K. Liu and X.G. Chen: *Metall. Mater. Trans. B*, 2015, vol. 47B, pp. 3291–3300.
4. Y.J. Li and L. Arnberg: *Acta Mater.*, 2003, vol. 51, pp. 3415–28.
5. R. Kamat: *JOM*, 1996, vol. 48, pp. 34–38.
6. Q. Du, W.J. Poole, M.A. Wells, and N.C. Parson: *Acta Mater.*, 2013, vol. 61, pp. 4961–73.
7. K. Liu, H. Ma, and X.G. Chen: *J. Alloys Compd.*, 2017, vol. 694, pp. 354–65.
8. K. Liu and X.-G. Chen: *J. Mater. Res.*, 2017, vol. 32, pp. 2585–93.
9. K. Liu, A.M. Nabawy, and X.-G. Chen: *Trans. Nonferrous Met. Soc. China*, 2017, vol. 27, pp. 771–78.
10. H.-W. Huang and B.-L. Ou: *Mater. Des.*, 2009, vol. 30, pp. 2685–92.
11. A.M.F. Muggerud, E.A. Mørtsell, Y. Li, and R. Holmestad: *Mater. Sci. Eng. A*, 2013, vol. 567, pp. 21–28.
12. Y. Li and L. Arnberg: *Essential Readings in Light Metal*, John Wiley & Sons, Inc., Hoboken, 2013, pp. 1021–27.
13. K. Liu and X.G. Chen: *Mater. Sci. Eng. A*, 2017, vol. 697, pp. 141–48.
14. Y.-L. Deng, Y.-Y. Zhang, L. Wan, A. Zhu, and X.-M. Zhang: *Metall. Mater. Trans. A*, 2013, vol. 44A, pp. 2470–77.
15. Z. Guo, G. Zhao, and X.G. Chen: *Mater. Charact.*, 2015, vol. 102, pp. 122–30.
16. Z. Jia, G. Hu, B. Forbord, and J.K. Solberg: *Mater. Sci. Eng. A*, 2008, vols. 483–484, pp. 195–98.
17. X.-Y. Lü, E.-J. Guo, P. Rometsch, and L.-J. Wang: *Trans. Nonferrous Met. Soc. China*, 2012, vol. 22, pp. 2645–51.
18. J.D. Robson: *Mater. Sci. Eng. A*, 2002, vol. 338, pp. 219–29.
19. P.X. Liu, Y. Liu, and R. Xu: *Trans. Nonferrous Met. Soc. China*, 2014, vol. 24, pp. 2443–51.
20. E.R. Weibel and H. Elias: *Quantitative Methods in Morphology*, Springer, Berlin, 1967.
21. A.R. Farkoosh, X.G. Chen, and M. Pekguleryuz: *Mater. Sci. Eng. A*, 2015, vol. 620, pp. 181–89.
22. L. Lodgaard and N. Ryum: *Mater. Sci. Eng. A*, 2000, vol. 283, pp. 144–52.
23. J. Osten, B. Milkereit, C. Schick, and O. Kessler: *Materials*, 2015, vol. 8, pp. 2830–48.
24. Y. Ohmori, L.C. Doan, and K. Nakai: *Nakai. Mater. Trans.*, 2002, vol. 43, pp. 246–55.
25. A. Gaber, M.A. Gaffar, M.S. Mostafa, and A.F. Abo Zeid: *Mater. Sci. Technol.*, 2006, vol. 22, pp. 1483–88.
26. L.C. Doan, K. Nakai, Y. Matsuura, S. Kobayashi *et al.*: *Mater. Trans.*, 2002, vol. 43, pp. 1371–80.
27. Y. Birol: *Trans. Nonferrous Met. Soc. China*, 2013, vol. 23, pp. 1875–81.
28. J.G. Kaufman: *Properties of Aluminum Alloys: Tensile, Creep, and Fatigue Data at High and Low Temperatures*, Aluminum Association, Washington, DC, 1999.
29. C. Booth-Morrison, D.C. Dunand, and D.N. Seidman: *Acta Mater.*, 2011, vol. 59, pp. 7029–42.
30. K.E. Knipling, D.C. Dunand, and D.N. Seidman: *Acta Mater.*, 2008, vol. 56, pp. 114–27.
31. X.M. Chen, Y.C. Lin, M.S. Chen, H.B. Li, D.X. Wen, J.L. Zhang *et al.*: *Mater. Des.*, 2015, vol. 77, pp. 41–49.
32. T. Wang, C. Wang, W. Sun, X. Qin, J. Guo, and L. Zhou: *Mater. Des.*, 2014, vol. 62, pp. 225–32.